AIAA JOURNAL
Vol. 40, No. 11, November 2002

Altering Turbulence in Compressible Base Flow Using Axisymmetric Sub-Boundary-Layer Disturbances

C. J. Bourdon* and J. C. Dutton†
University of Illinois at Urbana–Champaign, Urbana, Illinois 61801

The turbulent structures in the highly compressible near-wake region of a cylindrical base, to which an axisymmetric sub-boundary-layer strip disturbance has been applied, are examined in detail using a planar Rayleigh/Mie scattering visualization technique. When the downstream edge of the axisymmetric disturbance is placed approximately 12 momentum thicknesses upstream of the base termination, a base pressure increase of approximately 3% is noted over the no-tab case. The increased base pressure due to the presence of the axisymmetric disturbance is attributed to the transfer of turbulent energy into instability modes that are not supported in the near-wake region. Analysis of the large-scale turbulent structure visualizations indicates that, near the base, axisymmetric and low-order helical disturbances are present in the developing shear layer. This is indicated by a 35% increase in area-based and 20% increase in centroid-based unsteady motion in the end-view orientation, and a 100% increase in mean end-view structure size at the first imaging position, as compared to the no-tab case. As the shear layer travels downstream, the prominence of these disturbances is quickly diminished, due to the high convective Mach number (1.3) associated with the shear layer near the base. The centroid-based and area-based unsteady motion and end-view structure size all diminish to levels lower than those seen in the no-tab case and remain approximately constant throughout the remaining imaging positions.

I. Introduction

THE idea of modifying the trailing edge of splitter plates, nozzles, or afterbodies to alter the near-field mixing characteristics is not a new one. For instance, macroscopic point disturbances or tabs that extend far into the flow,[1,2] obstacles placed downstream,[3] afterbody boattailing,[4] and base bleed, ventilation, and base cavities[5] have all been employed with varying degrees of success. The presence of macroscopic obstacles can severely limit and/or alter the capabilities of a system. Drag-reducing mechanisms, such as afterbody boattailing or base bleed, also lead to significant alterations to a system's geometry and performance. The current study concentrates on a different type of drag- and mixing-altering mechanism, sub-boundary-layer disturbances, that can significantly alter the mixing characteristics of the base region of a separated flow without severely altering the afterbody/base geometry.

In the past, delta-shaped sub-boundary-layer disturbances have been implemented to enhance mixing in compressible planar shear-layer,[6] nozzle,[7] and base flowfields.[8] These studies show that sub-boundary-layer disturbances can potentially alter the evolution of a shear flow through the introduction of vorticity into the boundary layer before separation. It is even demonstrated that the vorticity generated from these structures will survive passage through the expansion fan present at the base corner separation point,[8] even though much of the organized turbulence present in the boundary layer is disrupted by the process.[9]

Strip disturbances have been introduced onto the trailing edge of splitter plates to introduce spanwise vorticity into a developing shear flow, thereby altering the mixing characteristics.[6] Introducing spanwise vorticity into compressible shear flows has proven to be relatively ineffective in improving the mixing characteristics of such flows and actually reduces the shear-layer thickness and growth rate in some cases.[6] Arnette et al.[10] attributed this to the inability of the compressible shear layer to amplify two-dimensional disturbances at large convective Mach number. It was also noted that the proximity of the two-dimensional disturbance to the edge of the splitter plate had a significant effect on the performance of any introduced disturbance. The work of Smith and Smits[11] on a Mach 2.9 boundary layer successively distorted by a 20-deg compression and a 20-deg expansion also suggests that a strip disturbance does not enhance mixing. Their study showed that, although the mean velocity profile had recovered by their last measurement position, approximately $20\delta_0$ downstream of the initial distortion, the Reynolds stresses were still decaying in the interior portion of the boundary layer.

Although strip disturbances have proven ineffective in enhancing mixing in compressible shear flows, there is still a benefit to examining their use in base flows. When base flows are examined, decreasing mixing (and, thus, increasing base pressure) without dramatically altering the afterbody can prove to have a large benefit. As Smith and Smits[11] demonstrated, multiple distortions of the boundary layer can lead to significant, quantifiable changes in the organization of the turbulent structures present in the boundary layer. Therefore, examining the effect that strip disturbances have on the evolution of turbulent structures present in the near wake can lead to improvements in passive and active control of compressible base flows.

Figure 1 presents a schematic of the unaltered near-wake flowfield of a supersonic base flow. The primary features of the near-wake region include an expansion fan emanating from the base corner separation point, compression waves that form as the outer flow approaches the symmetry axis, and a relatively strong recirculation region created by the low-momentum fluid in the base region that does not possess enough momentum to pass through the adverse pressure gradient formed by the recompression shock system. The turbulent structures examined in this study exist in the shear layer between the outer flow and recirculation or wake-core regions. These turbulent structures initiate the interaction between the recirculating fluid in the base region and the outer flow and, thus, control entrainment and mixing in the base region.

It is of critical importance to gain a more comprehensive understanding of the large-scale turbulent structures that dominate the developing wake region of compressible base flows. The role of the large-scale turbulent structures in the base region is particularly difficult to quantify because of the interaction that these structures have

Received 1 November 2001; revision received 7 June 2002; accepted for publication 25 June 2002.

*Graduate Research Assistant, Department of Mechanical and Industrial Engineering; currently Senior Member Technical Staff, Department of Experimental Thermal, Fluids and Aerosciences, Engineering Sciences Center, Sandia National Laboratories, P.O. Box 5800, MS 0834, Albuquerque, NM 87185. Member AIAA.

†W. Grafton and Lillian B. Wilkins Professor, Department of Mechanical and Industrial Engineering, 1206 West Green Street. Associate Fellow AIAA.

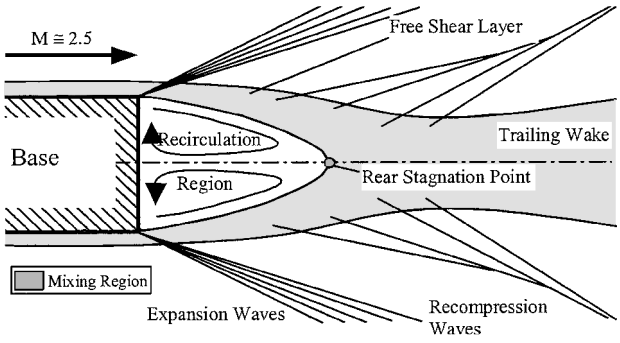

Fig. 1 Schematic of mean blunt-based flowfield.

with other features of the flowfield, such as the expansion fan emanating from the base corner and the compression waves that form as the shear layer approaches the axis of symmetry. These features introduce extra strain rates[12] to the flowfield, whose effects on the turbulence are nonlinearly coupled and, thus, are difficult to predict.

Most experimental studies of base flows have relied on pointwise measurement methods, such as laser Doppler velocimetry, to determine the turbulence statistics of the base region. Pointwise measurement techniques, although providing vital statistics, only capture the effect of the passage of large-scale turbulent structures and not the macroscopic nature of the structures themselves. Because of this shortcoming, our understanding of turbulence in compressible base flows is limited. In addition, more sophisticated turbulence models are necessary to capture truly the nature of compressible base flows in numerical computations, and, without experimental data that illuminate the features of the large-scale turbulence, the physics of such models will likely be flawed. When drag-altering mechanisms, such as the strip disturbances of the current study are examined, the role that large-scale turbulent structures play in determining the flowfield properties of the base region, such as the base pressure, mean velocity, and turbulence statistics, can be determined.

It is the objective of this study to provide such information through the use of planar visualization techniques. The effect of adding circumferential vorticity to the near-wake flowfield is observed here using a passive scalar Mie scattering planar visualization technique and is quantified using image averaging, spatial correlation analysis, and steadiness and shape factor analyses. These image-analysis techniques have been applied in planar[13] and axisymmetric[14–16] supersonic, compressible base flows without disturbances and yield a great deal of information about the evolution of the turbulent structures present in the near wake.

II. Facilities and Equipment

The axisymmetric, supersonic base-flow facility in the University of Illinois Gas Dynamics Laboratory was employed in this study. This is a blowdown-type wind tunnel, with compressed air supplied to the plenum chamber from an array of storage tanks that are filled by an Ingersoll–Rand compressor. The base model is supported by a 63.5-mm-diam sting that extends through the facility's supersonic converging–diverging nozzle. The freestream flow before separation from the base model is at a Mach number of 2.46, with a unit Reynolds number of 52×10^6 m^{-1}, at typical stagnation conditions of $P_0 = 368$ kPa and $T_0 = 300$ K. The turbulent boundary-layer thickness on the sting/afterbody just before separation has been measured to be 3.2 mm, and the momentum thickness is measured as 1 mm (Ref. 17).

The surface disturbances were formed in this study by application of pieces of adhesive shipping label to the surface of a blunt-based afterbody (Fig. 2). Disturbances as small as $\frac{1}{12}$ of the velocity deficit thickness have been found sufficient to produce asymmetries in overexpanded and ideally expanded jets.[18] In our facility, this translates to a disturbance thickness of approximately 0.1 mm (Ref. 19), the approximate thickness of the shipping label material. The disturbance thickness was altered by applying multiple layers of the labeling material. Because a large variety of tab configurations was examined, easy application and removal of the surface disturbances, as well as the cost of the disturbances, were key issues in choosing the tab material.

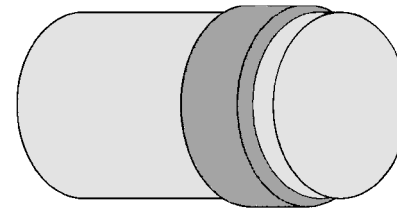

Fig. 2 Strip-tab configuration used in this study.

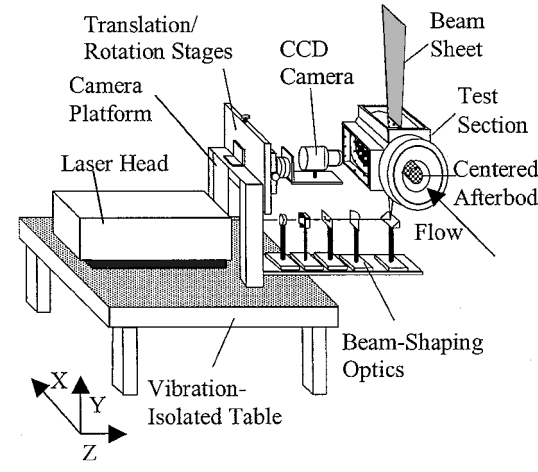

Fig. 3 Mie scattering image acquisition system.

For imaging data acquisition, the planar Rayleigh/Mie scattering technique was implemented in this study. In the past, this method has proved invaluable in visualizing and quantifying the turbulence structure of compressible shear flows.[8,13,14,20–22] Liquid ethanol is injected into the carrier air approximately 1.5 m upstream of the plenum chamber. The ethanol quickly evaporates as it is carried into the plenum. As the ethanol and carrier air are accelerated supersonically, the rapid expansion causes the vapor to condense into a fine mist, with a mean droplet diameter of approximately 0.05 μm (Ref. 23). This condensation occurs at thermodynamic conditions that correspond to a Mach number of approximately unity[23]; therefore, the interface between the supersonic outer flow and subsonic inner flow (recirculation or wake-core regions) is marked. A thin laser sheet, generated by a Nd:YAG laser, producing approximately 400 mJ per pulse at a frequency-doubled wavelength of 532 nm and with an 8-ns pulse width, illuminates the mist (Fig. 3). A 14-bit, back-illuminated, unintensified Photometrics charge-coupled device (CCD) camera is used to image the illuminated droplets.

III. Results and Discussion

Imaging positions have been chosen to correspond with key features in the flowfield. It is assumed that the locations of the mean reattachment point and the recompression shock system are approximately the same as for the blunt-based flowfield because the base pressure is increased only modestly by the strip disturbance. The imaging locations are described in Table 1 and shown in Fig. 4. Positions A and B correspond to the free shear-layer region of the flow, where pressure and extra strain rate effects are negligible. Position C is located in the center of the recompression region, where the outer flow begins to align itself with the symmetry axis. Position D is located at the mean reattachment point for the blunt-based case, and position E is in the developing wake region of the flow. The local convective Mach number of the shear layer, mean enclosed end-view area, and angle of the shear layer with respect to the symmetry axis are given for each imaging location in Table 1.

As mentioned earlier, the strip disturbance (Fig. 2) has been documented as not only being less effective at promoting mixing in planar shear layers, but actually decreases mixing in some cases.[6] It has also been noted that the proximity of the disturbance to the splitter

Table 1 Coordinates and estimated flow parameters at imaging positions

Imaging position	Location	Distance from base corner, mm	Convective Mach number[a]	End-view core area, A/A_{base}	Shear-layer angle, deg
A	Shear layer	18.4[b]	1.23	0.885	12.3
B	Shear layer	36.8[b]	1.40	0.690	13.3
C	Recompression	72.4[b]	1.24	0.280	7.8
D	Reattachment	84.1[c]	1.09	0.229	——
E	Near wake	135[c]	0.49	0.151	——

[a]Estimated. [b]Measured along shear layer. [c]Measured along centerline.

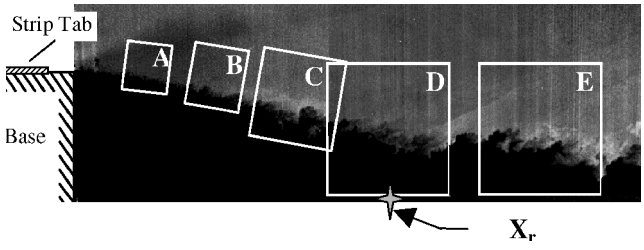

Fig. 4 Fields of view used in this study.

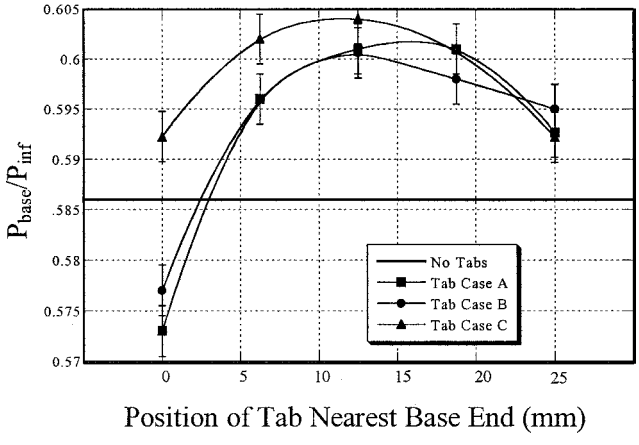

Fig. 5 Effect of strip tab on the base pressure of a cylindrical afterbody; case A tab is 12 mm wide, case B tab is 6 mm wide, and case C is two 6-mm-wide tabs placed 6 mm apart.

plate tip can significantly alter the mixing benefit or detriment of the disturbance generator.[6] Velocity measurements in supersonic boundary layers subject to multiple distortions show that, downstream of such disturbances, the Reynolds stresses do not recover in the inner portion of the boundary layer for at least 20δ (Ref. 11). Therefore, the true benefit of the strip tab could possibly be to decrease mixing and, thus, increase base pressure (reduce base drag) instead of increasing mixing.

A. Base Pressure Measurements

With this motivation, base-pressure data were acquired to quantify the effect that strip disturbances have on the drag characteristics of axisymmetric compressible reattaching flows. Three tab geometries were chosen: a single 12-mm-wide tab, a single 6-mm-wide tab, and a double tab, consisting of two 6-mm-wide tabs separated by 6 mm. The proximity of the trailing edge of the tab system to the base corner was varied from 0 to 25 mm. For all cases, the tabs were 0.5 mm thick. The results of the base pressure measurements as a function of tab position are shown in Fig. 5. All three cases demonstrate a base pressure maximum for a tab placement approximately 12 mm upstream of the base corner. The 12-mm-wide single tab (case A) produces a slightly higher base pressure than the 6-mm-wide single tab (case B), and the dual-tab configuration (case C) slightly outperforms either single-tab configuration. The optimal benefit of the strip disturbance for these thicknesses, widths, and tab placement can lead to a base pressure increase of 2.5–3.1%, without accounting for the increased drag caused by the disturbance itself.

B. Strip-Disturbance Visualizations

Because the maximum base-pressure increase of the strip disturbances is small, only the 12-mm-wide strip tab, located 12 mm from the trailing edge of the base (case A optimum), is examined in detail with the Rayleigh/Mie scattering technique. The effect of adding the strip disturbance is decidedly more difficult to see directly in the side- and end-view images than for the delta-shaped disturbances[8] examined earlier because the primary vorticity component created is circumferential instead of streamwise oriented. Therefore, large ensembles of images have been obtained in both the side and end views so that statistics can be derived to quantify the effect that the strip disturbance has on the turbulent structures of the near wake. As in previous studies of this type,[13–16] five imaging locations have been chosen to represent the different stages in the development of the shear layer in the near wake. Ensembles of 500 images have been gathered at each imaging position and in both the side and end views. It has been shown previously that ensembles of this size are sufficient to produce stable statistics.[13]

Instantaneous images from the near-wake region of the axisymmetric reattaching flow altered by a strip disturbance are presented in Fig. 6. Average images are not presented because the ensemble-averaged shear layer does not contain any significant features. As in the no-tab case, the shear layer is circular and symmetric in the average end view, indicating that there is no significant, stationary, streamwise-oriented structure. Qualitatively, the instantaneous images seem very similar in character to those of the no-disturbance base flowfield. The differences lie in the organization and apparent activity of the turbulent structures visible along the interface. In the side view (Fig. 6a, most obvious in bottom image), the structures appear often to be regularly spaced, a feature rarely seen in the no-tab case. This suggests that there may be a periodic shedding of the turbulent structures from the strip tab. The other feature that differentiates these images from the no-tab case is that, like images from the near wake of a boattailed afterbody,[16] the tortuousness and variability of the individual structures appears to be lower than in the no-tab case. The border between the freestream and core fluid contains more gray scales and fewer serrated and/or jagged edges.

The average 10–90% intensity shear-layer thickness at each imaging position is presented in Fig. 7. These results show that the shear layer is thicker through the mean reattachment point due to the presence of the strip disturbance. The shear-layer growth rate displays a significantly different behavior, however. In the strip-tab

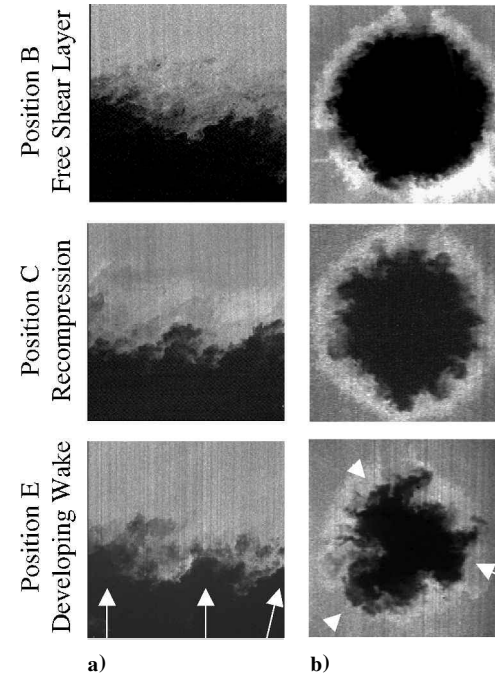

Fig. 6 Selected imaging positions in near-wake region of strip-tab disturbed flow: a) instantaneous side and b) end views; arrows indicate the approximate location of turbulent structure centers.

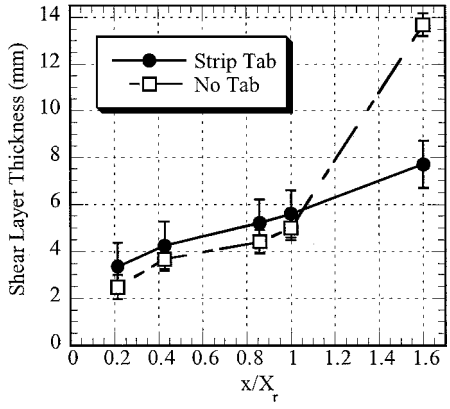

Fig. 7 Average shear-layer thickness for 12-mm-wide tab, located 12 mm upstream of base corner.

case, the growth rate near the base is slightly lower, indicating lower entrainment rates and, thus, higher base pressure (Fig. 5) (Refs. 14 and 17). The shear-layer growth rate, interestingly, is virtually constant throughout the near-wake region for the strip-disturbance case. This indicates that the adverse pressure gradient and streamline curvature effects that promote an increased growth rate in the no-tab case do not affect the strip-tab near wake in the same fashion. The most readily apparent difference between the strip and nondisturbed cases is the proximity of the shear-layer interface to the centerline (closer for no tabs). The mean core fluid area actually reaches a minimum in the reattachment region[15] for the no-tab case. Therefore, streamline convergence effects can be deduced as responsible for the change in slope apparent in Fig. 7 for the no-tab case at the mean reattachment point. The diminished influence of streamline convergence and the absence of concave streamline curvature in the strip-disturbed flowfield near reattachment leads to diminished shear-layer growth rates in the developing wake region and a much thinner shear layer at imaging position E.

C. Shape Factor

As defined in this study, the shape factor is the ratio of the actual length of an interface to the theoretical minimum interface length. For example, when an enclosed interface, such as the shear layer seen in the current end views is examined, the minimum interface length would be the circumference of a circle encompassing the same area. For an open interface, such as seen in the current side views, the minimum interface length would be that of a straight line connecting the most upstream and downstream boundary points. The shape factor is intended to be an indication of the mixing potential of a given interface.

The side- and end-view shape factor values calculated for the strip-tab and no-tab cases[15] are presented in Figs. 8 and 9, respectively. For Figs. 8 and 9, the interface is defined as the location where the intensity is 20% of the freestream value. The shape factor values are insensitive to the choice of the interface intensity value because the intensity gradient between the freestream and recirculating fluid is generally very sharp. These shape factor results are the means of approximately 500 shape factor values for each image ensemble, and the uncertainty bars on the measurements represent the rms values calculated for the ensemble at each imaging location. In general, shape factor variability is higher in the side view than in the end view. This effect is related both to the dominant orientation of the large-scale structures and to the side-view and end-view window sizes.[15] Because the major axis of the large-scale structures is generally oriented in the streamwise direction, the variability of individual turbulent structures leads to a higher variability in the side view than in the end view. The field of view is approximately three times the size of individual turbulent structures in the side view and is much larger in the end view. Thus, in the side view, the passage of individual structures through the field of view can contribute significantly to the calculated rms shape factor value. In the end view, there are more structures present in each image frame, and the contribution to the rms shape factor value from individual turbulent structures is smaller.

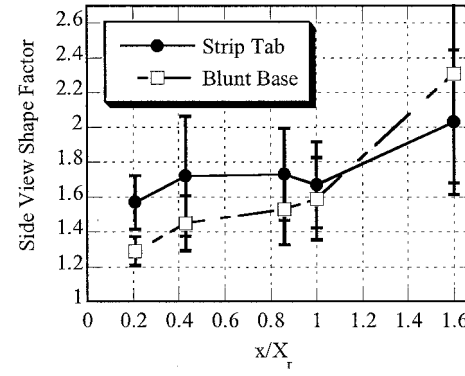

Fig. 8 Side-view shape factor for strip-tab case.

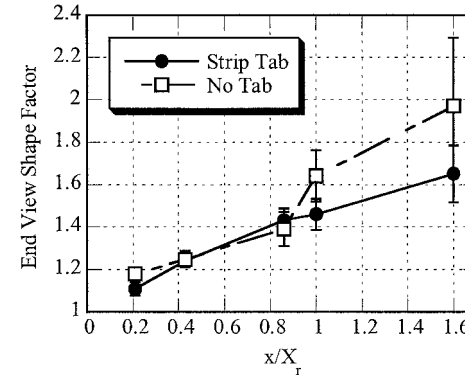

Fig. 9 End-view shape factor for strip-tab case.

Several interesting trends are seen in Figs. 8 and 9. First, the shape factor appears to change very little between imaging locations B and C and then decreases between C and D in the side view (Fig. 8) for the strip-tab case. This decreasing trend, although small, indicates that there is little mixing or development occurring near reattachment in the strip-disturbed near wake. At position A, near the base, the side-view shape factor is markedly higher for the strip-disturbed flowfield than for the nondisturbed flowfield. However, at the mean reattachment point, position D, the shape factor values are approximately equal. Another noteworthy difference between the strip-disturbed and nondisturbed flowfields is apparent in the end view (Fig. 9) at position D, the mean reattachment point. In the no-tab case, there is a jump in the end-view shape factor value from that at position C due to the impingement of the shear layer on the centerline and the three-dimensional nature of the reattachment process.[15] For the strip tab-disturbed flow, there is no change in the rate of increase of the end-view shape factor at this position. This indicates that the streamline curvature and axisymmetric confinement effects seen in the no-tab case[15] do not generate the same type of mixing at the mean reattachment point for the strip-tab case. The final result of interest is seen in the last imaging position in the developing wake. Because of the lower pressure rise due to the higher base pressure in the strip-disturbed case than in the no-tab case, the mixing enhancement that recompression causes is much smaller, and the shape factors are much lower downstream as a result.

D. Steadiness/Flapping Motions

The unsteady nature of the shear layer is determined from a statistical examination of the interface between the freestream and core fluids in the instantaneous images. The interface is designated here as the location where the scattered light intensity drops to 20% of the freestream value. The shear-layer position (normal to the streamwise direction) in each instantaneous side-view image can be compared with that of the entire ensemble, and bulk shear-layer motion can, thus, be detected. In the end view, the shear layer is nominally a circular, closed curve. Because of this, both pulsing (or expansion/contraction) and flapping (or centroidal) motions can be described. This technique is described in detail in Ref. 15.

If the assertions of other researchers[6,10] can be extended to the current work, several key patterns should be visible in the steadiness and flapping analysis of the strip-tab case. First, one would expect the overall level of shear-layer motion to increase from the no-tab case. In Smith and Smits's work,[11] it was shown that the Reynolds stresses in the inner portion of the boundary layer were much lower after successive distortions. When the Reynolds stresses, which indicate the level of organized turbulent motions in a flow, are small, the reattaching shear layer should be more prone to pulsing and/or flapping types of motion, especially near the base. Second, due to the spanwise vorticity promoted by the strip disturbance, it is expected that pulsing or axisymmetric motions will again be larger near the base. Such instability modes are not naturally enhanced in flows with such a large convective Mach number (~1.3 near the base; Table 1) as the current flow, and so this enhanced motion should be quickly damped. Third, the circumferential vorticity generated by the strip tab should help to enforce flow symmetry. The back-and-forth "sloshing" motions that were present in the no-tab case[15] in the recompression region (position C) and developing wake (position E) are not expected to be as strongly organized in the strip-tab results. These sloshing motions evident in the no-tab case were determined to be an artifact of the either the wind-tunnel facility or a slight scratch or defect on the blunt base and not truly a feature of the flowfield. The strip disturbance should produce a much larger perturbation than this artifact.

The results of the steadiness analysis are presented in Figs. 10–12. As expected, both area-based (Fig. 10) and centroidal motions (Fig. 11) are 20–30% higher at position A for the strip-tab case. Therefore, axisymmetric and low-order helical instability modes are generated by the strip disturbance. This leads to an almost 50% increase in apparent flapping motions seen in the side view at this position (Fig. 12). These enhanced motions are quickly damped, however, leading to dramatically lower levels of fluctuations by position B, the second imaging position. From position B to the last imaging position (position E), both area-based (Fig. 10) and centroidal (Fig. 11) fluctuations remain at lower levels than are seen at imaging position A. In the side view, the shear-layer motion indicates something slightly different (Fig. 12). The flapping motions for the strip-tab base are damped between positions A and B but still remain higher at position B than for the no-tab case. From position B downstream to position E, the variation of the flapping motions of the strip-tab case mirror those of the no-tab case, but are about 3–5% of the local shear-layer thickness larger. The difference can be attributed to two factors. First, the area-based fluctuations seen in Fig. 10 persist at a relatively high level throughout the recompression (position C) and reattachment (position D) regions in the strip-tab case. In the recompression and reattachment regions, the area fluctuations (which contribute to evident side-view flapping) are approximately twice as large for the strip-tab case as the no-tab case. Second, the sloshing motions observed in the no-tab case at positions C and E are not indicated in the side-view measurements because they were based on the preferential passage of the turbulent structures in the end view along the Z axis (Fig. 3), and the side-view statistics are based on information along the Y axis. Therefore, the statistics presented for the no-tab side-view flapping motions are slightly lower than the mean apparent radial flapping motions.

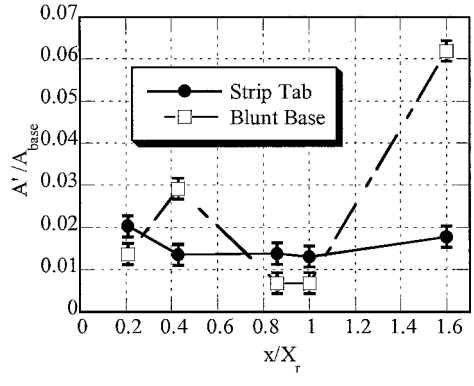

Fig. 10 End-view area fluctuations seen in near wake of strip-tab flowfield.

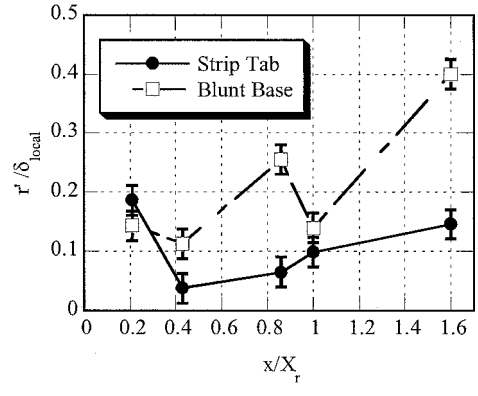

Fig. 11 End-view centroid motion seen in the near wake of strip-tab flowfield.

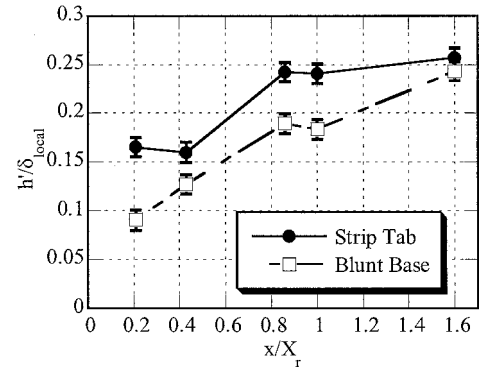

Fig. 12 Side-view flapping motions seen in near wake of strip-tab flowfield.

E. Spatial Correlation Analysis

A spatial correlation analysis technique is employed to estimate the mean size, shape, and orientation of the turbulent structures present in the shear layer. The images acquired in this study were of relatively low intensity, occupying only 10% of the dynamic range of the CCD. Therefore, an intensity-averaging technique[24] was employed to increase the fidelity of the statistics gathered from the raw images. The dynamic range of each image frame has been normalized such that the mean freestream intensity value is the same, and the mean background intensity is zero. For a more detailed description of this technique, see Ref. 24. This reduces the intensity variations caused by variations in the seeding levels and laser sheet intensity, thus reducing the noise level in the correlation field.

The spatial correlation fields at all five imaging positions for the strip-tab case are presented for the side view in Fig. 13. The frames are oriented such that the horizontal axis is parallel to the symmetry line of the near wake, and the vertical side of each frame has a length equal to one local shear-layer thickness. The features of these contours are qualitatively similar to those of the no-tab case. In the free shear layer, positions A and B, the turbulent structures (based, as in previous studies, on the 0.5 correlation contour[13,14]) occupy approximately one-half of the shear-layer thickness, and are inclined at approximately 45 deg from the mean shear-layer direction. In the recompression and reattachment regions, positions C and D, the structures become strained, stretching well over a shear-layer thickness in length and rotating to a shallow angle with respect to the shear layer. In the wake region, position E, the turbulent structures relax back to a shape akin to those of the initial imaging positions.

Another feature, rotation of the interior contour levels with respect to the outer contour, is also present in the correlation fields of the strip-disturbed case at positions B, C, and D. It has been postulated that this rotation of the inner contours occurs in regions of the flow where destabilizing influences act on the peripheries of the structures.[23] In the no-tab case,[14] inner-contour rotation is evident at positions B and C, whereas for the boattailed case,[16] it was evident

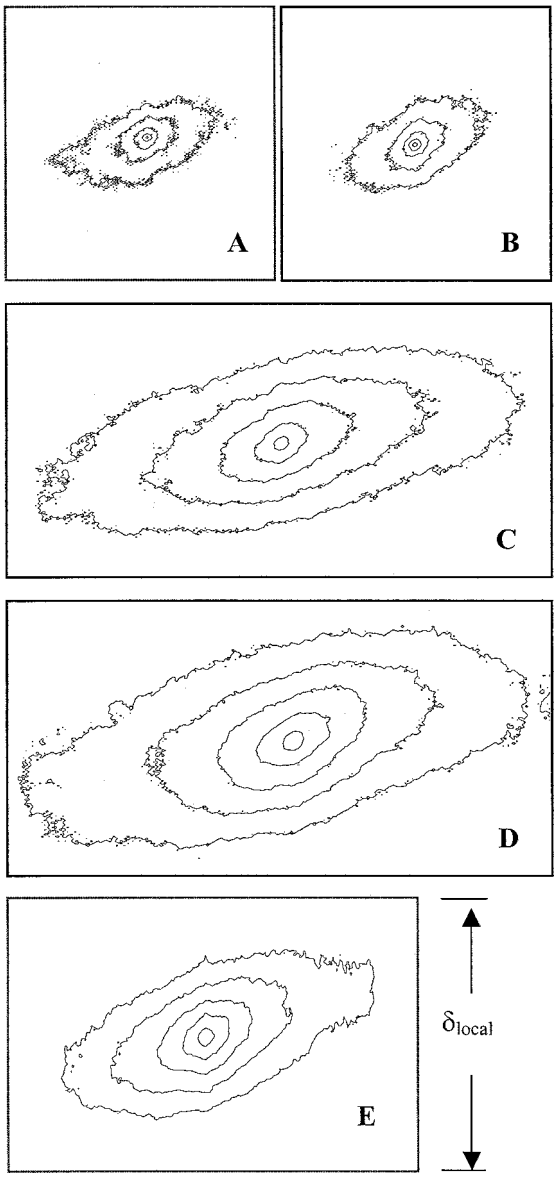

Fig. 13 Side-view spatial correlation fields at imaging positions A–E for strip-tab case; contours are at 0.1 intervals from 0.5 to 0.9.

at positions C and D. The present results are, thus, consistent with these previous findings. Lack of inner-contour rotation at position B for the boattailed afterbody was attributed to the weakened influence of the adverse pressure gradient for this flow geometry. Conversely, the contour rotation evident at the mean reattachment point, position D, for the boattailed afterbody was attributed to the diminished influence of lateral streamline convergence (a stabilizing influence) due to the longer reattachment length and higher base pressure. The current strip-disturbed flowfield displays an increase in base pressure that is less significant than in the boattailed afterbody case. Therefore, a hybrid situation exists; the recompression process is strong enough to be evident here, leading to contour rotation at position D.

The end-view spatial correlation fields for imaging positions A–E are presented in Fig. 14. The correlation contours are oriented such that the freestream is at the top of the frame, while the recirculation/wake core region is at the bottom, and flow is out of the page. Aside from imaging position A, the mean structure is slightly elliptical, with the long axis pointing from the core fluid region to the freestream. The mean structure at position A, however, displays a much different character. Because of the increased flapping and/ or axisymmetric pulsing motions generated by the strip disturbance (due to increased circumferential vorticity), the mean structure occupies a circumferential span of approximately two shear-layer thicknesses. The high convective Mach number near the base dictates that spanwise structures will not remain coherent

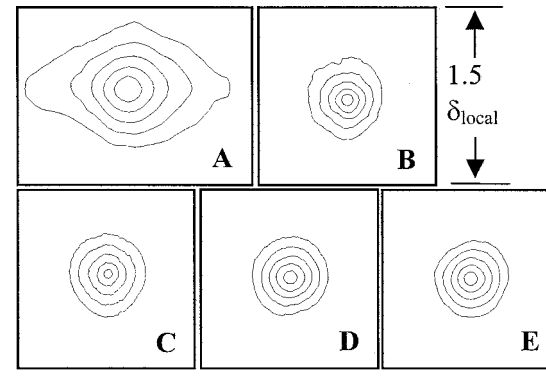

Fig. 14 End-view spatial correlation fields for strip-tab case; contours are at intervals of 0.1 from 0.5 to 0.9.

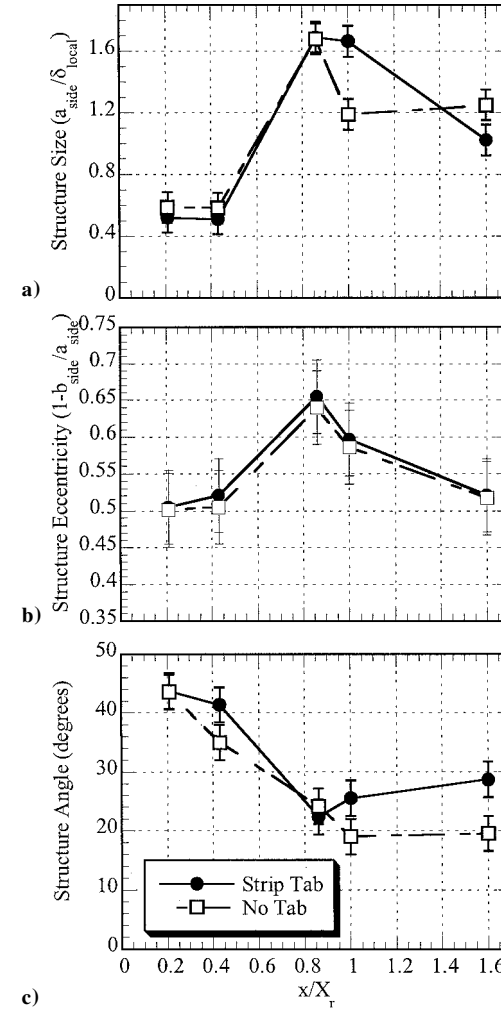

Fig. 15 Side-view correlation statistics at imaging locations A–E for strip-tab case and comparison with no-tab case.

and, thus, there is no trace of this spanwise dominance at position B or further downstream.

Figure 15 presents the primary statistical results of the correlation analysis in the side-view orientation for both the strip-disturbed and no-tab flowfields.[14] The lengths of the major and minor axes of the mean large-scale structures correspond to the symbols a and b, respectively. The structure angle is defined as the angle of the structure's major axis a to the local shear-layer direction. The results are qualitatively similar for the two cases, especially before the mean reattachment point ($x/X_r = 1$).

In the initial portions of the developing shear layer, the mean large-scale structures grow at a rate approximately equal to the growth rate of the shear layer, while maintaining a relatively constant eccentricity and rotating down toward the streamwise axis. The

structure-angle near the base (Fig. 15c) is actually slightly larger for the strip-tab case than for the no-tab case. This is in contrast to the side-view correlation results for the boattailed base flowfield,[16] in which the side-view structure angle is consistently lower than for the no-tab case. For the boattailed afterbody, it was suggested that, due to the decreased structure angle in this region, less interfacial area was available for entrainment and mixing, leading to higher base pressure and lower base drag. From the structure-angle measurements presented here, it is seen that the mechanism causing higher base pressure in the strip-tab case is slightly different. The diversion of turbulent energy into enhanced flapping motions near the base (Fig. 12), which does not actively promote mixing, may be responsible for the higher base pressure in this case.

The first significant deviations in the side-view correlation results presented for the no-tab and strip-tab results are seen at the mean reattachment point. The mean structure size is substantially higher for the strip-tab case than for the no-tab case, and the mean structure angle actually increases from the value in the recompression region, rather than decreasing, as in the no-tab case. Both of these features can be attributed to the proximity of the shear layer in this region to the centerline (Table 1). In the no-tab case,[14] the end-view core area approaches a minimum value of approximately 12% of the base area in this region. For the strip-tab case, the end-view core area at the mean reattachment point is 23% of the base area. Because of this, interaction across the centerline and axisymmetric confinement effects are much less significant for the strip-tab case. These effects were deemed responsible for the rapid decrease in structure size in the no-tab case, and so it is plausible that their diminished role in the strip-tab base flow accounts for this difference in size.

Statistical results from the end-view correlation analysis are presented in Fig. 16. The most distinctive features of these results are present at the first imaging location. Because of the axisymmetric mode promoted by the strip disturbance, the correlation statistics indicate that a large and eccentric mean structure, oriented along the shear-layer circumference, is present at the first imaging position (position A). Refer to Fig. 14. The axisymmetric disturbance is quickly damped, however, and the dimensionless mean structure size approaches a constant value of about 0.65 at the remaining measurement locations. This result is to be expected in a highly compressible flowfield. Unlike incompressible or weakly compressible shear layers, the low-order helical and axisymmetric instability modes no longer contain the most energy and decay faster than higher-order modes.[25] The structure size appears to be unaffected by the adverse pressure gradient and reattachment processes at positions C and D. The structure eccentricity stays approximately constant (within measurement accuracy) and slightly above zero for all imaging positions after the first.

The ratio of end-view to side-view major axes (Fig. 16c), which is an indicator of the preferential organization of the turbulence,[23] indicates that, after the first imaging position, the same trends are apparent with and without the strip-tab disturbance. The initial spanwise dominance of the structures for the strip-tab geometry is quickly damped due to the high convective Mach number of the shear layer. The strip tab results actually indicate a slightly smaller circumferential-to-streamwise aspect ratio of the mean structures for the strip-tab base for all imaging positions after the first. Also, due to the diminished role that the adverse pressure gradient (due to higher base pressure), streamline convergence, and cross-centerline interaction have in the reattachment region, the turbulent structures in this region tend to relax and "stand up" in relation to the local flow direction.

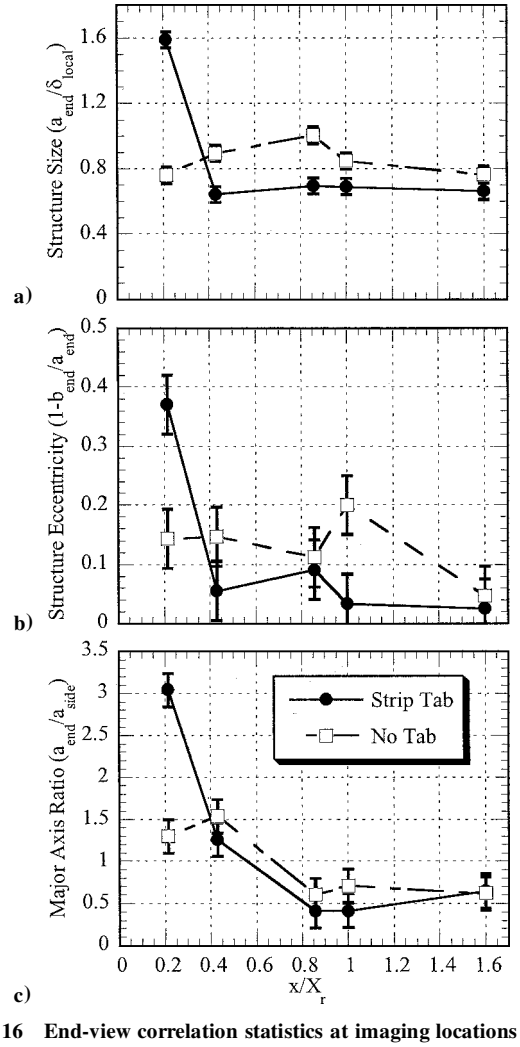

Fig. 16 End-view correlation statistics at imaging locations A–E for strip-tab case and comparison with no-tab case.

IV. Summary

This work demonstrates that axisymmetric sub-boundary-layer surface disturbances can significantly alter the mixing and drag characteristics of the base region in a compressible, reattaching, axisymmetric flow. The disturbances accomplish this by altering the turbulence structure in the base region.

Axisymmetric-strip disturbances are shown to enhance both axisymmetric (area-based pulsing) and centroidal shear-layer motion near the base, without significantly altering the mean turbulence structure evident in the side view. This symmetric motion enhancement leads to a large, circumferentially eccentric end-view structure at the first imaging position. Because of the large convective Mach number in the near-wake region, this enhanced flapping motion, and end-view mean structure shape is quickly damped. Because the circumferentially oriented structures generated by the strip tab are damped so quickly, the base pressure actually increases by up to 3%.

Interestingly, the presence of the axisymmetric sub-boundary-layer disturbances had little effect on the turbulent structure statistics at downstream imaging positions. Turbulent structure generation caused by the separation of the boundary layer from the base and passage through the base corner expansion fan does not appear to be influenced by the presence of the strip disturbances at these locations.

Acknowledgments

This work was supported by the U.S. Army Research Office (ARO) under Grant DAAD19-01-1-0367. The support of ARO and this project's Technical Monitor, Thomas L. Doligalski, are gratefully acknowledged.

References

[1]Wishart, D. P., Krothapalli, A., and Mungal, M. G., "Supersonic Jet Control via Point Disturbances Inside the Nozzle," *AIAA Journal*, Vol. 31, No. 7, 1993, pp. 1340, 1341.

[2]Glawe, D. D., Samimy, M., Nejad, A. S., and Chen, T. H., "Effects of Nozzle Geometry on Parallel Injection into a Supersonic Flow," *Journal of Propulsion and Power*, Vol. 12, No. 6, 1996, pp. 1159–1168.

[3]Raman, G., and Rice, E. J., "Supersonic Jet Mixing Enhancement Using Impingement Tones from Obstacles of Various Geometries," *AIAA Journal*, Vol. 33, No. 3, 1995, pp. 454–462.

[4]Viswanath, P. R., and Narasimha, R., "Two-Dimensional Boat-Tailed Bases in Supersonic Flow," *Aeronautical Quarterly*, Vol. 25, No. 3, 1974, pp. 210–224.

[5]Viswanath, P. R., and Patil, S. R., "Effectiveness of Passive Devices for Axisymmetric Base Drag Reduction at Mach 2," *Journal of Spacecraft and Rockets*, Vol. 27, No. 6, 1990, pp. 234–237.

[6]Island, T. C., Urban, W. D., and Mungal, M. G., "Mixing Enhancement in Compressible Shear Layers via Sub-Boundary Layer Disturbances," *Physics of Fluids*, Vol. 10, No. 4, 1998, pp. 1008–1020.

[7]King, C. J., Krothapalli, A., and Strykowski, P. J., "Streamwise Vorticity Generation in Supersonic Jets with Minimal Thrust Loss," AIAA Paper 94-0661, Jan. 1994.

[8]Bourdon, C. J., and Dutton, J. C., "Mixing Enhancement in Compressible Base Flows via Generation of Streamwise Vorticity," *AIAA Journal*, Vol. 39, No. 8, 2001, pp. 1633–1635.

[9]Herrin, J. L., and Dutton, J. C., "Effect of a Rapid Expansion on the Development of Compressible Free Shear Layers," *Physics of Fluids*, Vol. 7, No. 1, 1995, pp. 159–171.

[10]Arnette, S. A., Samimy, M., and Elliott, G. S., "The Effects of Expansion on the Turbulence Structure of Compressible Boundary Layers," *Journal of Fluid Mechanics*, Vol. 367, 1998, pp. 67–105.

[11]Smith, D. R., and Smits, A. J., "Multiple Distortion of a Supersonic Turbulent Boundary Layer," *Applied Scientific Research*, Vol. 51, No. 1–2, 1993, pp. 223–229.

[12]Bradshaw, P., "The Effect of Mean Compression or Dilatation on the Turbulence Structure of Supersonic Boundary Layers," *Journal of Fluid Mechanics*, Vol. 63, No. 3, 1973, pp. 449–464.

[13]Smith, K. M., and Dutton, J. C., "Investigation of Large-Scale Structures in Supersonic Planar Base Flows," *AIAA Journal*, Vol. 34, No. 6, 1996, pp. 1146–1152.

[14]Bourdon, C. J., and Dutton, J. C., "Planar Visualizations of Large-Scale Turbulent Structures in Axisymmetric Supersonic Separated Flows," *Physics of Fluids*, Vol. 11, No. 1, 1999, pp. 201–213.

[15]Bourdon, C. J., and Dutton, J. C., "Shear-Layer Flapping and Interface Convolution in a Separated Supersonic Flow," *AIAA Journal*, Vol. 38, No. 10, 2000, pp. 1907–1915.

[16]Bourdon, C. J., and Dutton, J. C., "Effects of Boattailing on the Turbulence Structure of a Compressible Base Flow," *Journal of Spacecraft and Rockets*, Vol. 38, No. 4, 2001, pp. 534–541.

[17]Herrin, J. L., and Dutton, J. C., "Supersonic Base Flow Experiments in the Near Wake of a Cylindrical Afterbody," *AIAA Journal*, Vol. 32, No. 1, 1994, pp. 77–83.

[18]Krothapalli, A., Strykowski, P. J., and King, C. J., "Origin of Streamwise Vortices in Supersonic Jets," *AIAA Journal*, Vol. 36, No. 5, 1998, pp. 869–872.

[19]Herrin, J. L., "An Experimental Investigation of Supersonic Axisymmetric Base Flows Including the Effects of Afterbody Boattailing," Ph.D. Dissertation, Dept. of Mechanical and Industrial Engineering, Univ. of Illinois at Urbana–Champaign, Urbana, IL, July 1993.

[20]Clemens, N. T., and Mungal, M. G., "A Planar Mie Scattering Technique for Visualizing Supersonic Mixing Flows," *Experiments in Fluids*, Vol. 11, No. 2, 1991, pp. 175–185.

[21]Elliott, G. S., Samimy, M., and Arnette, S. A., "The Characteristics and Evolution of Large-Scale Structures in Compressible Mixing Layers," *Physics of Fluids*, Vol. 7, No. 4, 1995, pp. 864–876.

[22]Messessmith, N. L., and Dutton, J. C., "Characteristic Features of Large Structures in Compressible Mixing Layers," *AIAA Journal*, Vol. 34, No. 9, 1996, pp. 1814–1821.

[23]Smith, K. M., "The Role of Large Structures in Compressible Reattaching Shear Flows," Ph.D. Dissertation, Dept. of Mechanical and Industrial Engineering, Univ. of Illinois at Urbana–Champaign, Urbana, IL, Aug. 1996.

[24]Smith, K. M., and Dutton, J. C., "Procedure for Turbulent Structure Convection Velocity Measurements Using Time-Correlated Images," *Experiments in Fluids*, Vol. 27, No. 3, 1999, pp. 244–250.

[25]Tourbier, D., and Fasel, H., "Numerical Investigation of Transitional Axisymmetric Wakes at Supersonic Speeds," AIAA Paper 94-2286, Jan. 1994.

J. P. Gore
Associate Editor